Recent Developments in Snow-Chemistry Research in the Western United States

R.E. DAVIS

U.S. Army Cold Regions Research and Engineering Laboratory
72 Lyme Road
Hanover, New Hampshire 03755-1290, U.S.A.

R.C. BALES

Department of Hydrology and Water Resources
University of Arizona
Tucson, Arizona 85221, U.S.A.

ABSTRACT

Three active areas of detailed research in snow and ice chemistry will be described with emphasis on the connection between processes at different scales: i) modeling chemical hydrographs from seasonal snowpacks in alpine watersheds, ii) studying processes affecting ion redistribution in, and elution from snow, and iii) investigating the interaction of trace gases in snow. First, in alpine watersheds where snowmelt runoff dominates basin hydrology, accurate hydrochemical modeling depends on developing adequate descriptions of snowmelt chemistry. Whole-watershed hydrochemical modeling using point descriptions of snowmelt chemistry, along with distributed estimates of snowmelt volume, is being pursued for the Emerald Lake (Sierra Nevada) and other alpine watersheds in the western U.S. Second, tracer studies at the Sierra Nevada Aquatic Research Laboratory are being used to develop point estimates of snowmelt volume versus chemistry for use in the distributed watershed models. Complimentary field studies are ongoing at the U.S. Forest Service's Glacier Lakes site in Wyoming, and the Mammoth Mountain (California) field site of the University of California, Santa Barbara. Third, recent studies by researchers at the University of Arizona and the U.S. Forest Service have used chromatographic methods to examine the interaction of reactive gases (SO_2, H_2O_2) with ice surface, continuing earlier investigations of gaseous deposition to snow.

CHEMICAL HYDROGRAPH FROM ALPINE SNOWPACKS

Whole-watershed studies at Emerald Lake (Sequoia National Park) of California's Sierra Nevada (Williams and Melack, 1989, 1990) and at the Glacier Lakes Experimental Eocosystem Site (GLEES) in the Snowy Range of Wyoming (Clow et al., 1988) have identified ionic pulses in the first fractions of streamflow during spring melt. Williams and Melack (1989) show that sampling the chemistry of all subbasins in a watershed is necessary to adequately characterize solute inputs to lake systems. Furthermore, they show a case in which spatial and temporal variations in the melt over the watershed do not change the magnitude of the solute pulse, rather, they extend the pulse duration. The importance of melt-freeze cycling is pointed out by Williams and Melack (1990), who showed that increased concentrations of solutes in meltwater can be associated with a series of melt-freeze cycles. Snowpack and lake monitoring is continuing at several sites in the Sierra Nevada under the California Air Resources Board monitoring program. At GLEES the ionic pulse was less distinct and soil contributions to lake-inflow chemistry appeared to be quite important (Clow et al., 1988). Studies by the University of Wyoming and the U.S. Forest Service are continuing at GLEES, which the Forest Service plans to use as a long-term ecological research site.

Figure 1 shows data from Williams and Melack (1990) for snowpack and meltwater concentrations of major ions over time, showing the initial high concentration factor of the initial melt. This figure also shows another large ionic pulse starting on April 23 after a series of melt-freeze cycles. While the ionic pulse starting on April 23 follows a series of preceding melt-freeze cycles, the cycles themselves may not be the direct cause. Instead it may be the lack of continued melt flow diluting the concentrations of species in solution. Figure 2 shows a time series of the movement of SO_2 and NO_3^- down through the pack at the same site. In this figure in high concentrations are seen near the base of the pack, where the ions will be

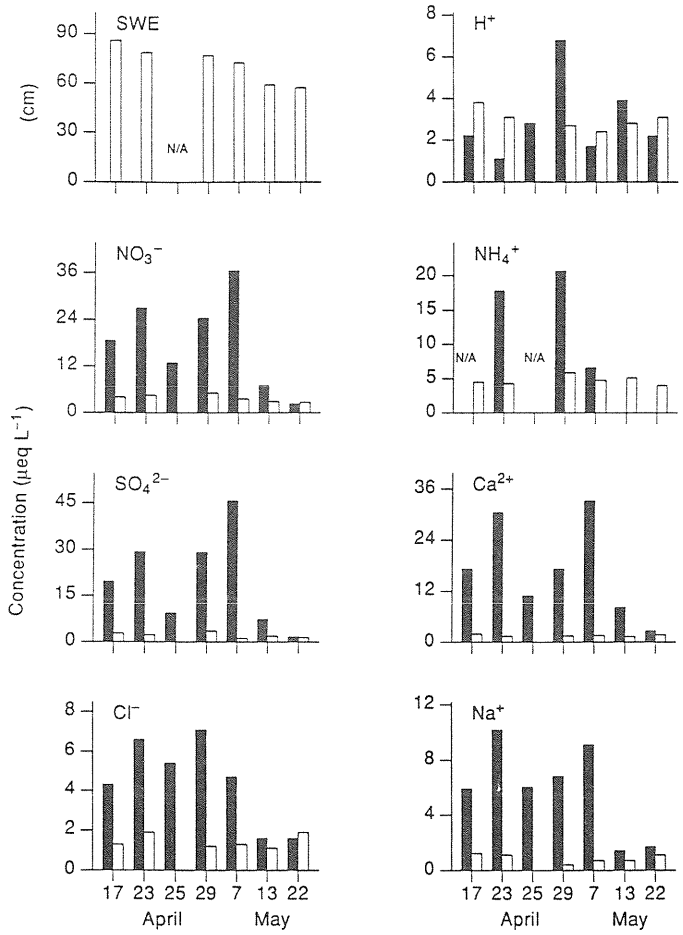

Figure 1. Snow water equivalent and the concentration of major ions in the snowpack (clear bars) and in the snowpack meltwater (black bars) at a sub-basin in the Emerald Lake watershed, California, in 1987. Solute concentrations in the initial melt fraction are higher than the bulk snowpack concentrations. Solutes increased in concentration around April 23, after a series of melt-freeze events, and the increase in concentration on April 29 is due to rainfall *(After Dozier and Melack, 1989)*.

removed at the onset of new melt flow. This condition was previously described in a laboratory setting by Colbeck (1980).

Whole-watershed hydrochemical modeling using point descriptions of snowmelt chemistry, along with distributed estimates of snowmelt volume, is being pursued for the Emerald-Lake and other alpine watersheds in the western U.S (Wolford et al., 1988; Sorooshian et al., 1989). Figure 3 shows a partial division of the Emerald Lake watershed into sub-basins, and the measured chemical and flow hydrographs for three lake inflows. Each inflow is an aggregation of runoff from multiple sub-basins. The chemical hydrograph at any scale, from a single point to the whole basin, can be empirically fit with this three-parameter exponential expression

$$\frac{C}{C_a} = \frac{d\,MF}{d\,VF} = \alpha b_1 e^{-b_1 VF} + (1-\alpha) b_2 e^{-b_2 VF} \qquad (1)$$

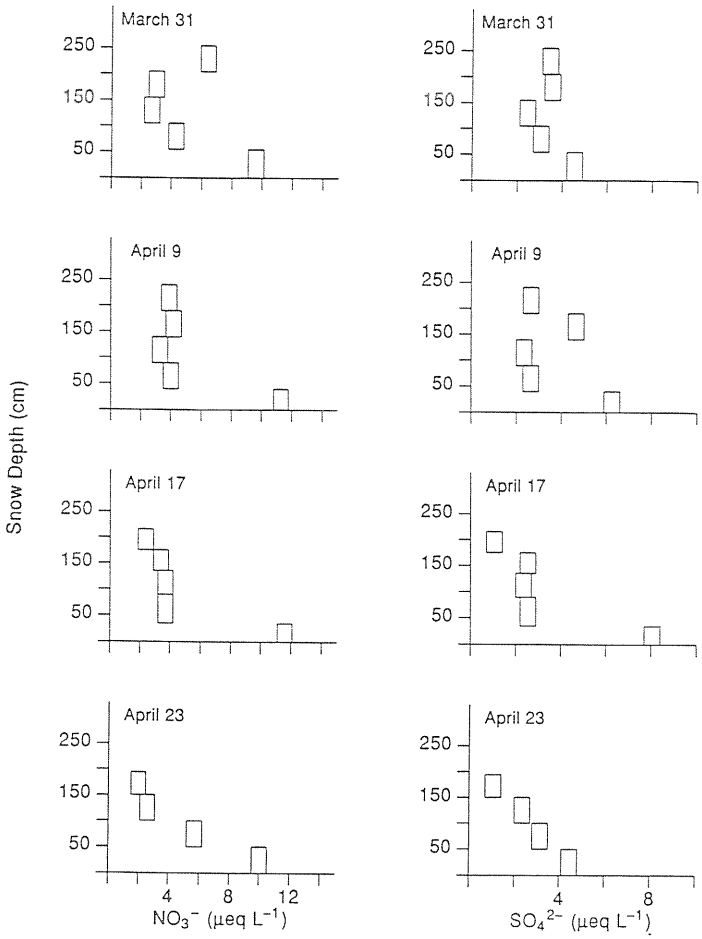

Figure 2. A time series of the concentrations of two major ions, NO_3^- and SO_2 at the same site in the Emerald Lake watershed in 1987. The concentrations near the top of the declining pack decrease over time while the concentrations near the bottom of the pack increase *(After Dozier and Melack, 1989)*.

where

α	weighting parameter (0 – 1)
b_1 and b_2	empirical parameters
VF	volume fraction of melt
C_a	average initial in snowpack
C	concentration of meltwater draining from pack

Integrating the above equation, obtains the mass fraction MF eluted

$$MF = \alpha\left[1 - e^{-b_1 VF}\right] + (1 - \alpha)\left[1 - e^{-b_2 VF}\right] \quad (2)$$

When one aggregates snowmelt from several points that melt at different times, the aggregated chemical hydrograph should have a significantly lower peak than a point estimate (Figure 4). Note that the initial peak *observed* will depend on what volume fraction of snowmelt is sampled. Williams and Melack (1990) point out that the pulse was not much reduced when the flows from multiple sub-basins were measured,

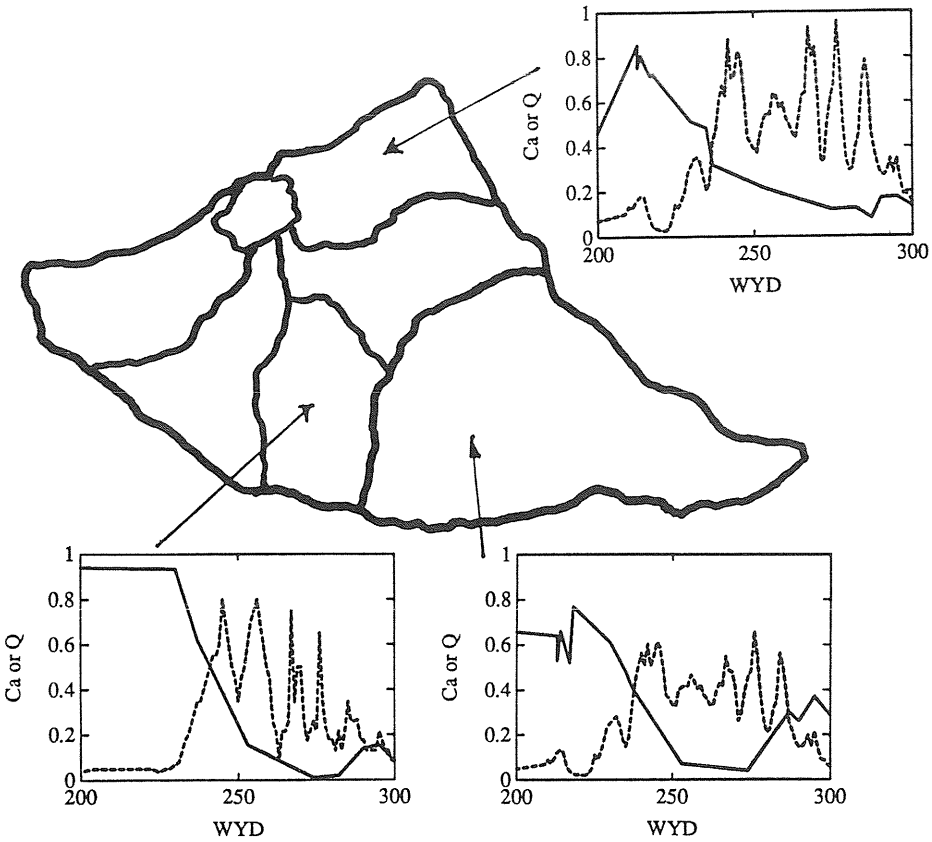

Figure 3. Chemical (dashed line) and melt (solid line) hydrographs for three inflows to Emerald Lake watershed, and an example of hydrologic subdivisions; for hydrochemical modeling, subdivisions are divided based on runoff, snow accumulation and melt, and soil-vegetation types.

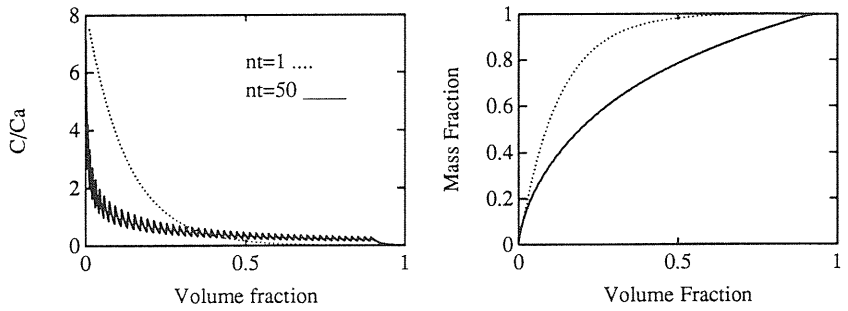

Figure 4. Example chemical hydrograph for one point and for 50 contributing points, each lagged in time for the previous one by 10 percent of the volume at that point. Axes are a) snowmelt concentration divided by the (initial) average in the pack as a function of fraction of the snowpack melted, and b) cumulative mass fraction released as a function of fraction melted.

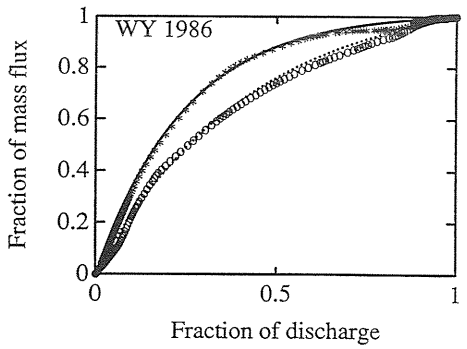

Figure 5. Chemical hydrographs for two Emerald Lake inflows, 1986 water year. Data are for NO_3^-, based on daily flow values and weekly chemistry sampling. These are basically integrals of the chemical hydrographs shown in Figure 3.

however, suggesting that the aggregation on Figure 4 should be over fewer points. Figure 5 shows the fraction of solute mass flux reaching the lake inflow as a function of the fraction of snowmelt discharge, pointing out the differences in melt patterns over the watershed.

Ongoing laboratory studies at the Sierra Nevada Aquatic Research Laboratory (SNARL), which is operated by the University of California, Santa Barbara (UCSB), field studies at the U.S. Forest Service's GLEES site, and field studies at Mammoth Mountain, California (UCSB) are aimed towards developing point estimates of ion concentrations in meltwater for use in the distributed watershed models. The point-based model being initially tested and extended is from Hibberd (1984), and the mass balance of the solutes is given by

$$\frac{\partial C_i}{\partial t^*} + (S + \beta)\left[\frac{\partial C_m}{\partial t^*} + u^* \frac{\partial C_m}{\partial z^*}\right] = (S + \beta) D^* \frac{\partial^2 C_m}{\partial z^{*2}} \tag{3}$$

where

C_i	mass concentration solute in immobile phase
C_m	mass concentration solute in mobile phase
S	effective saturation of the pore space
β	$= \frac{S_i}{1 - S_i}$
S_i	irreducible liquid water content
u^*	percolation velocity
D^*	dispersion coefficient
t	time
z	vertical distance coordinate

The flux u^* is obtained using Colbeck's (1978) theory. Two alternative chemical models may be used to relate C_i and C_m

$$\frac{\partial C_i}{\partial t} = K \frac{\partial C_m}{\partial t} \tag{4}$$

or

$$\frac{\partial C_i}{\partial t} = k_1 (C_m - C_i) \tag{5}$$

where K is a partion coefficient, and k_1 is a first order kinetic release coefficient. Work to develop mathematical descriptions of snowmelt chemistry at a point is in progress (Bales and Davis, manuscript in preparation), to go along with efforts at developing a distributed snowmelt model (Marks and Dozier, 1988).

In a laboratory study, Bales et al. (1989a) observed that the initial ionic distribution at both the mesoscale and microscale influence relative concentrations in solute released from the pack. Figure 6 shows the vertical profiles of SO_4^{2-} and Br^- measured at intermediate and late stages of melting; the SO_4^{2-} was applied to the top of the pack and the Br^- to the middle. Tracers applied at the top of the pack come out before those at depth, with 80 percent of the species at the top removed in first 20 percent of meltwater (Figure 7). For a mid-depth tracer, 70 percent of solute mass was removed in first 20 percent of meltwater.

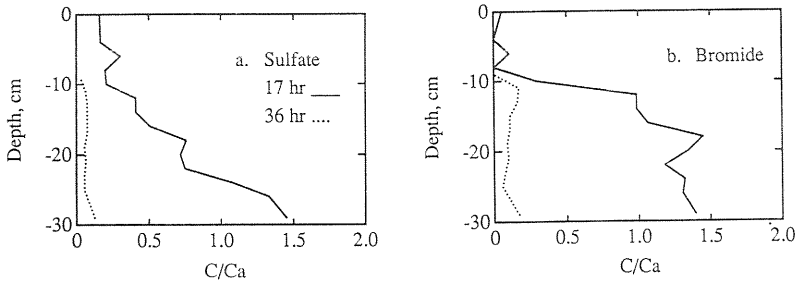

Figure 6. Solute profiles at two times during melting of a laboratory snowpack. Conditions: 1 × 1 × 0.4 m snowpack; ρ = 370 kg m^{-3}; tracers applied, top: 1 L of 0.04 M NaBr and mid: 1 L of 0.05 M KCl, HNO_3 and Na_2SO_4; melt rate = 0.66 cm hr^{-1}; 57 percent of pack melted in 34 hr (Bales et al., 1989).

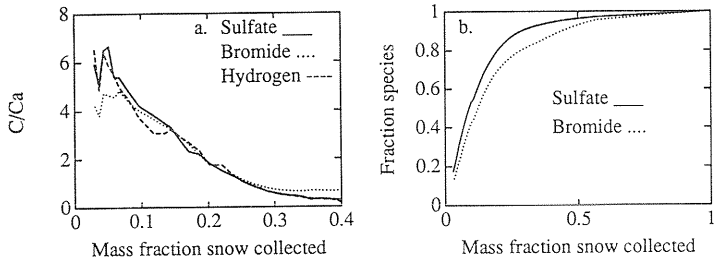

Figure 7. Solute release for same experiment as Figure 6: a) cumulative mass of ionic mass released as a function of fraction of snowpack melted in cold-room experiments, b) chemical hydrograph for release of SO_4^{2-}, H^+ and Br^- from a snowpack.

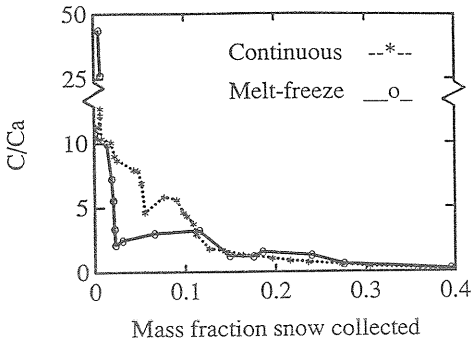

Figure 8. Chemical hydrograph from melting of laboratory snowpack; conditions similar to those of Figure 7, except that three melt-freeze cycles were imposed prior to final melting.

However, results also show that there is partial mixing and an important *immobile* region on snow grains; some of top tracer comes out late and some of mid-depth tracer comes out in the first meltwater (Bales et al., 1989a). There was no *preferential* elution of three different salt tracers applied at the top of the pack; all arrived together in meltwater (Figure 7). Figure 8 shows the effect of melt-freeze cycles compared with continuous melt; the melt freeze cycles result in an ionic pulse much larger in amplitude than the case of continuous melt. This shows that melt-freeze cycles can also cause a stronger ionic pulse from initially dry snowpacks, in this case it results from the concentration of solutes on less grain surface. The melt-freeze process causes grains to grow rapidly and solutes to be flushed from interstices, more readily leached.

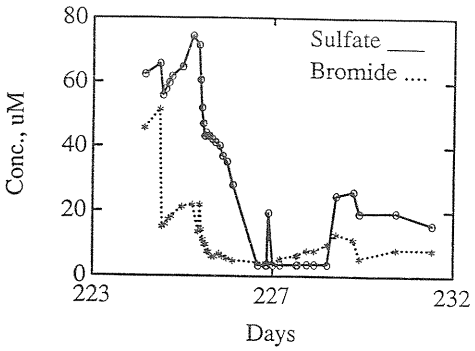

Figure 9. Meltwater concentrations for one lysimeter at the Glacier Lakes field site. Snowpack depth was ~2 m (Bales et al, 1990).

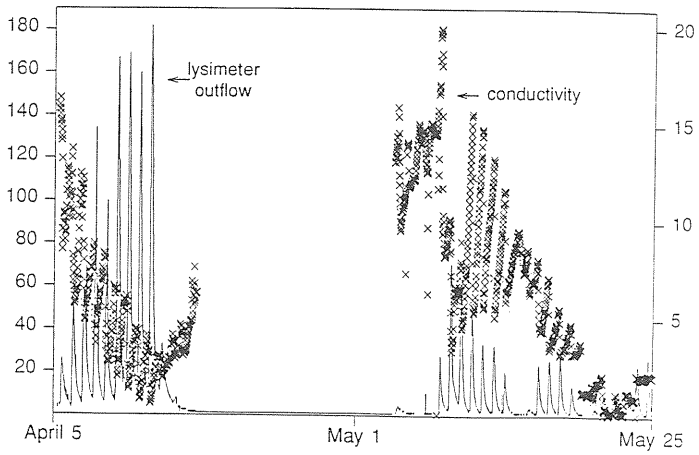

Figure 10. Measurements from lysimeters at the Mammoth Mountain snow study plot. Daily melt hydrographs are show for two melt episodes; the associated chemical hydrographs are shown with measurements of meltwater conductivity. In each case a pulse in concentration is seen at the onset of melt arrival at the base of the pack.

Figure 9 shows an ionic pulse of four to ten times the average snowpack concentration in snow lysimeters at GLEES, observed on the first day of melt, with both background ions and tracers showing a peak (Bales et al., 1990). Snow pits showed solute depletion from the base and possible additions to the top of the pack during melt. Figure 10 shows the results of tracer tests at Mammoth Mountain, California, in which the daily hydrographs are shown, averaged from a pair of lysimeters, along with the conductivity of the melt water. This shows a sharp peak at the start of the first melt episode, followed by a period of subfreezing surface conditions, then a higher peak when melt flow resumes to the base of the pack.

ION REDISTRIBUTION IN AND ELUTION FROM SNOW

Besides contributing data for developing point estimates of ion release from melting snowpacks, the studies at the Mammoth-Mountain and Glacier lakes field sites and at SNARL are investigating process-level questions concerning ion redistribution in snow. Detailed observations are being made of snow stratigraphy and chemistry in controlled field plots. For example, the 2-m snowpack at Glacier lakes showed rapid initial melt (2 cm dy^{-1}), but most of the tracer mass applied directly above the lysimeters was diverted away by ice lenses and preferential flow paths. In neither lysimeter or snow-pit data for 1988 was there a clear relation between stratigraphy and chemistry, however (Bales et al., 1990). Two further sets of measurements for 1989 and 1990 are being analyzed.

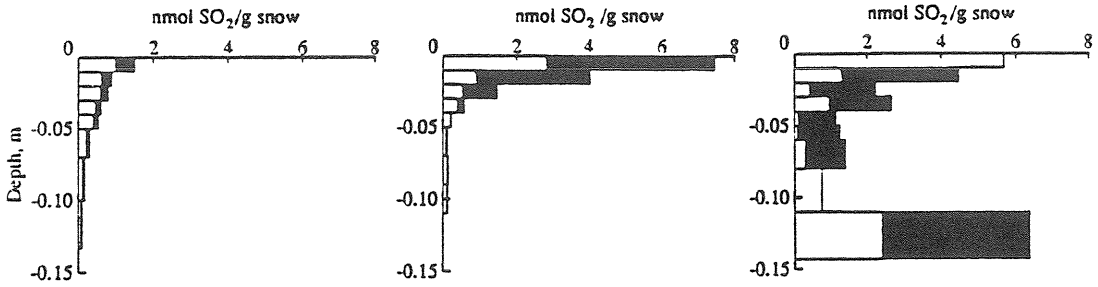

Figure 11. Depth profiles of HSO_3^- and SO_4^{2-} in snow. SO_2 gas in the air above the snow diffused down into the pack, and was taken up in the liquid water on the surface of the snow grains.

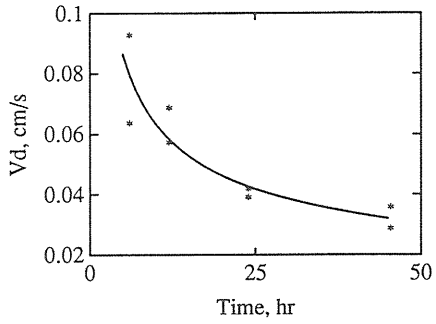

Figure 12. SO_2 deposition velocity to snow as a function of time. Experimental conditions: –0.5°C, SO_2 at ~25 ppbv (*After Conklin, 1988*).

INTERACTION OF TRACE GASES WITH SNOW

Recent studies have looked at the uptake of SO_2 and NO_x by snow and ice and the presence of trace species such as H_2O_2 in snowpacks.

There is both thermodynamic and indirect experimental evidence for a disordered interfacial region on ice at temperatures below 0°C. This surface *liquid-like* region is related to surface roughening, depends on facets, and is stable above ~20°C. One example of this phenomenon is the increased adsorption of SO_2 onto ice from -11 to -3°C observed in studies carried out at Desert Research Institute, Reno, NV (Sommerfeld and Lamb, 1986). Ongoing studies with ice spheres show that uptake of NO exhibits a similar temperature dependence *[R. Sommerfeld, unpublished data, U.S. Forest Service, Fort Collins, CO.]*

Experimental studies (Valdez et al., 1987) and mathematical modeling (Bales et al., 1987) of SO_2 deposition show that snow acts as a perfect, though diffuse, sink for reactive gases. The major factor determining the deposition velocity (flux to surface divided by atmospheric concentration) is the liquid-water content of the snow (Figure 11). Measured deposition velocities averaged 0.06 cm s^{-1}, with values of 0.02 cm s^{-1} for cold, dry, old snow; 0.05 cm s^{-1} for cold, dry, new snow (greater surface area); and 0.07 cm s^{-1} for wet, old snow. Ozone and SO_2 concentrations did not affect deposition velocity (Valdez et al., 1987). The diffusive transport and reaction model for SO_2 uptake compared well with experimental results, with liquid-water mass fraction being the main parameter. The model also predicted that deposition velocity should drop with time because the pH of the surface liquid layer drops as more SO_2 is taken up; SO_2 solubility decreases at lower pH because it is an acid (Bales et al., 1987). Later experiments provided validation to this predicted time dependence (Figure 12). Further studies in progress are aimed at a quantitative validation of how uptake depends on oxidant concentration *[M. H. Conklin, unpublished data, U. Arizona].*

Valdez et al. (1989) observed that SO_2 uptake onto growing ice surfaces at -15°C was in amounts equivalent to Henry's law equilibrium between the gas phase and deposited H_2O. This is consistent with uptake into a 10-100 nm liquid-like layer at the growing interface, with SO_2 release inhibited by diffusion in the layer. At equilibrium, SO_2 should be largely excluded from the ice.

Hydrogen peroxide is an important oxidant in some alpine and polar regions and has been found to be stable in snow and ice. Concentrations in snow pits and in fresh snow from the Sierra Nevada and Snowy Range are on the order of a few $\mu g L^{-1}$ and show decreases with depth (time), however *[M. H. Conklin, manuscript in preparation, U. Arizona].*

SUMMARY

Similar relationships between meltwater hydrographs and chemical hydrographs are seen at the watershed scale, a point scales, and in the laboratory. For the most part, chemical hydrographs peak during the rising limb of the meltwater hydrograph, which shows the importance of understanding snowpack processes early in the ablation season. To understand these relationships at the process level, we must first examine the microscale phenomena that are responsible for the distributions of solutes that control uptake and transport by liquid water. Next, we must identify water flow processes in snow that affect the removal of species from various parts of the snowcover. Finally we need to integrate the knowledge of these processes to account for a variety of flow paths at the watershed scale.

REFERENCES

Bales, R. C., R. E. Davis and D. A. Stanley, Ionic elution through shallow, homogeneous snow, *Water Resources Research,* 25, 1869-1877, 1989.

Bales, R. C., R. A. Sommerfeld and D. G. Kebler, Ionic tracer movement through a Wyoming snowpack, *Atmospheric Environment, (In press),* 1990.

Bales, R. C., M. P. Valdez and G. A. Dawson, Gaseous deposition to snow: II. Physical-chemical model for SO_2 deposition, *Journal of Geophysical Research,* 92, 9789-9799, 1987.

Clow, D. C., N. Swoboda-Colberg, J. I. Drever, and F. S. Sanders, Chemistry of snowmelt, soil water, and stream water at the West Glacier lake watershed, Wyoming, *EOS,* 69, 1198, 1988.

Conklin, M. H., Time dependence of SO_2 dry deposition to snow, *EOS,* 69, 1053, 1988.

Marks, D., and J. Dozier, Climate and energy exchange at the snow surface in the alpine region of the Sierra Nevada, *EOS,* 69, 1213, 1988.

Sommerfeld, R. A. and D. Lamb, Preliminary measurements of SO_2 adsorbed on ice, *Geophysical Research Letters,* 13, 349-351, 1986.

Sorooshian, S., R. C. Bales, V. K. Gupta, P. A. Noppe, and R. A. Wolford, Development of Watershed Models for Emerald Lake Watershed in Sequoia National Park and Other Lakes of the Sierra Nevada, *Draft final report for the California Air Resources Board on contract A732-035,* University of Arizona, Tucson AZ, 217 p., 1989.

Valdez, M. P., R. C. Bales, D. A. Stanley, and G. A. Dawson, Gaseous deposition to snow: I. Experimental study of SO_2 and *no* 2 deposition, *Journal of Geophysical Research,* 92, 9799-9789, 1987.

Valdez, M. P., G. A. Dawson, and R. C. Bales, Sulphur dioxide incorporation into ice depositing from the vapor, *Journal of Geophysical Research,* 94, 1095-1103, 1989.

Williams, M. W., and J. M. Melack, Effects of spatial and temporal variation in snow melt on nitrate ion and sulphate ion pulses in melt waters within an alpine basin, *Annals of Glaciology,* 13, 285-288, 1989.

Williams, M. W., and J. M. Melack, Solute chemistry of snowmelt runoff in an alpine basin, Sierra Nevada, *Water Resources Research, (In press),* 1990.

Wolford, R. A., S. Sorooshian, R. C. Bales, and G. A. Dawson, A hydrochemical and water balance model for Emerald Lake watershed, Sierra Nevada, California, *EOS,* 69, 1199, 1988.